Soft Matter

PAPER

View Article Online
View Journal | View Issue

Cite this: *Soft Matter*, 2022, **18**, 7236

Self-regulating electrical rhythms with liquid crystal oligomer networks in hybrid circuitry†

Mert O. Astam,[ab] Pengrong Lyu,[ab] Jacques Peixoto[ab] and Danqing Liu *[abc]

Self-regulation is an essential aspect in the practicality of electronic systems, ranging from household heaters to robots for industrial manufacturing. In such devices, self-regulation is conventionally achieved through separate sensors working in tandem with control modules. In this paper, we harness the reversible actuating properties of liquid crystal oligomer network (LCON) polymers to design a self-regulated oscillator. A dynamic equilibrium is achieved by applying a thermally-responsive and electrically-functionalized LCON film as a dual-action component, namely as a combined electrical switch and composite actuating sensor, within a circuit. This hybrid circuit configuration, consisting of both inorganic and organic material, generates a self-regulated feedback loop which cycles regularly and indefinitely. The feedback loop cycle frequency is tunable between approximately 0.08 and 0.87 Hz by altering multiple factors, such as supplied power or LCON chemistry. Our research aims to drive the material-to-device transition of stimuli-responsive LCONs, striving towards applications in electronic soft robotics.

Received 17th August 2022,
Accepted 9th September 2022

DOI: 10.1039/d2sm01117d

rsc.li/soft-matter-journal

Introduction

Automated production lines running series of self-regulating robots is a defining image of modern industry. Feedback-loop-based appliances, functioning without human input, enhance our comfort and efficiency beyond what was imaginable in the past.[1] In both productivity and relaxation, self-regulation is a significant contributor to our quality of life.[2] The conventional perception of self-regulation manifests in sensors coupled with control modules.[3] However, state-of-the-art electronic systems still cannot match the highly sustainable, integrated and responsive self-regulating systems observed in nature.[4] The biological human heart is one such system, capable of continuously operating for decades while being fully responsive to environmental changes and feedback from its complimentary organs.[5] The high complexity of this system is reflected by the ongoing efforts of the medical field in replicating a biological human heart.[6] A major challenge in this aspect of the field is achieving an integrated feedback loop, where the device must pulse actuate with a variable frequency in response to changing environmental conditions.[7] This complex self-regulating behaviour requires a highly-integrated or, more ideally, a compliant single-material device with actuator, sensor and control module functions.[8] A single electronic component that is mechanically compliant and can perform all three functions to achieve self-regulation has currently not been conceived.[9] Nevertheless, one may venture for solutions to this challenge in the active field of soft materials. This field historically offers a broad potential for applications due to the compliant nature of soft materials, which entails prospects for superior biomimicry.[10] Therefore, soft material applications are pursued in fields requiring precise functions, such as in the medical field.[11] The practicality of such soft materials is further elevated by its adaptation to advanced additive manufacturing methods.[12] In the case of self-regulation, the proven sensing capabilities and programmable actuation of stimuli-responsive soft materials are formidable.[13–15]

Liquid crystals (LCs) first sparked interest with their tuneable anisotropic optical properties.[16] They are best known for their application in display technology, namely liquid crystal displays (or LCDs).[17] Yet, the anisotropic properties of LCs also translate into readily functionalized particles and highly tuneable mechanical and stimuli-responsive actuation in liquid crystal networks (LCNs).[18–24] The emerging functions of LCNs are especially applicable in biomimicking soft robotics because the compliant nature and stimuli-responsive actuation of the material allows for robotic functions in restrictive environments.[25]

[a] *Laboratory of Stimuli-Responsive Functional Materials and Devices (SFD), Department of Chemical Engineering and Chemistry, Eindhoven University of Technology, Groene Loper 3, 5612 AE Eindhoven, The Netherlands. E-mail: d.liu1@tue.nl*
[b] *Institute for Complex Molecular Systems (ICMS), Eindhoven University of Technology, Groene Loper 3, 5612 AE Eindhoven, The Netherlands*
[c] *SCNU-TUE Joint Lab of Device Integrated Responsive Materials (DIRM), National Center for International Research on Green Optoelectronics, South China Normal University, Guangzhou 510006, China*

† Electronic supplementary information (ESI) available. See DOI: https://doi.org/10.1039/d2sm01117d

Therefore, researchers have replicated natural systems with LCNs, such as artificial muscles or swimmers.[26,27] In these studies, LCNs have been explored in the form of free-standing films or fibres, where the material gains the capacity to bear load as well as actuate. This is particularly interesting for soft robotics as it demonstrates the integration of two robotic functions within a single-material component.[28] Yet, the impact of this functional integration can be elevated by exploiting the stimuli-responsiveness-based intrinsic sensing capabilities of LCNs towards building self-regulated systems.[29–31] This would make a functional machine out of the LCN material itself which overarches all the robotic functions, including sensing, responding, actuating and doing work to maintain a set state. Eventually, we envision these self-regulating functions in LCNs would replicate those observed in nature, even in electrically-stimulated systems such as the biological human heart.

In this work, we demonstrate the electrically-driven self-regulating potential of liquid crystal oligomer networks (LCONs) by building a free-film oscillator. LCONs were selected due to the greater molecular mobility possible in oligomer chain networks than in long-chain, glassy networks typical to LCNs. As a result, LCONs can undergo greater deformation compared to LCNs, while exerting similar actuation forces.[32] This allows LCONs to operate the oscillator continuously and without tearing or rupturing. Dynamic equilibrium is achieved by using an electrically-functionalized LCON film in a circuit as a composite actuating sensor for automated electrical switching. Through Joule heating, the thermally-responsive LCON film is actuated, opening the circuit. The subsequent cooling of the LCON film leads to material relaxation and closing of the circuit. Magnets are integrated into the device to set a threshold between on- and off-phases. This hybrid circuit, now consisting of both inorganic and organic material, generates a feedback loop which cycles indefinitely with minimal shifts in frequency or free-film amplitude. The feedback loop cycle frequency (FLCF) is tuneable by altering the power supplied to the device, while the chemistry of the LCON and the flux profile of the integrated magnets can be varied to influence both FLCF and free-film oscillation amplitude. Consequently, our oscillator incorporates the actuating, load-bearing, control and sensing mechanisms into a single overarching LCON component to achieve tuneable self-regulation.

Results and discussion

Oscillator self-regulation and feedback loop mechanism

The self-regulating abilities of the stimuli-responsive LCON film are initiated by the ''two-phase'' feedback loop design of our oscillator. Fundamentally, the oscillator enters its off-state when the actuation of the film breaks the circuit, while the on-state is reinstated when the LCON relaxes back to its initial dimensions. (Fig. 1A and Videos S1, S2, ESI†) The distinctness of the on- and off-states is crucial in the oscillator operation, thus the conductive nichrome heating element is fastened to the LCON film to prevent continued heating in the off-state. (Fig. 1B) Yet, simply isolating the on- and off-states electrically cannot induce a distinction. Operating the device with this initial configuration would lead to the LCON film being suspended in a specific position where the electrical contact is exactly sufficient to maintain equilibrium. This electrical contact would correspond to the heating rate and equilibrium temperature that is needed to actuate the film to this position. Consequently, no sustained oscillation would be recorded with this configuration. The issue with this set-up is the electrical contact not being fully broken upon LCON actuation. A hard phase difference between the on- and off-states is missing. In our oscillator design, we establish this phase difference by uncoupling the actuation stress and strain behaviours of the LCON film. This is achieved by mounting one magnet on the film and one within the device platform. (Fig. 1C) In the on-state of the device, the magnets compress the LCON film to the device platform with a force equivalent to their magnetic attraction. This restricts the actuation strain of the LCON film and induces an internal tension build-up instead. The internal tension, or actuation force, of the LCON film must reach a certain magnitude to overcome the attraction force between the mounted magnets and subsequently break contact with the oscillator platform. Fundamentally, the magnetic attraction force acts as an actuation force threshold for the LCON, thereby inducing a phase difference between on- and off-states of the oscillator. The exact magnitude of the internal tension needed to overcome the actuation force threshold is subject to geometric factors, as annotated for the case of our oscillator in Fig. 1D. Hence, static mechanics was used to calculate the $2T\sin(0.806) > M$ actuation force criteria for the device to enter the off-state, where T denotes the tension within the LCON film and M denotes the force of attraction between the mounted magnets. In the case of our oscillator design, the magnetic attraction force (M) was equivalent to approximately 323 mN. Upon entering the off-state, the actuation strain of the LCON is no longer restricted and the residual internal tension translates into the corresponding strain, as this is the energetically favourable state for the system. The stress to strain conversion within the system is near-immediate, which causes the LCON film to snap outwards and away from the device platform. This movement also reduces the attractive force between the mounted magnets to a negligible magnitude. The magnets were chosen as such that the magnetic flux profile entails rapid decrease in attraction force with distance, reducing magnetic interferences in the motion of the LCON film after the oscillator enters its off-state. (Fig. 1E) In the off-state, the absence of Joule heating allows the LCON film to cool down and reverse its actuation. Eventually the film will make contact with the oscillator platform again, re-entering its on-state and triggering a repeat of the process. This establishes a clear ''two-phase'' feedback loop that is regulated by the properties of the LCON film.

Square signal generation

The ''two-phase'' feedback loop of the self-regulating oscillator is mirrored by the voltage changes recorded in the test circuit (Fig. 1F). An oscilloscope was attached to the voltage-dispensing diodes in the test circuit and a signal akin to a square wave was recorded during oscillator operation. The minima of the square wave correspond to the off-state and *vice versa* (Fig. 1G). The overall feedback-loop cycle frequency

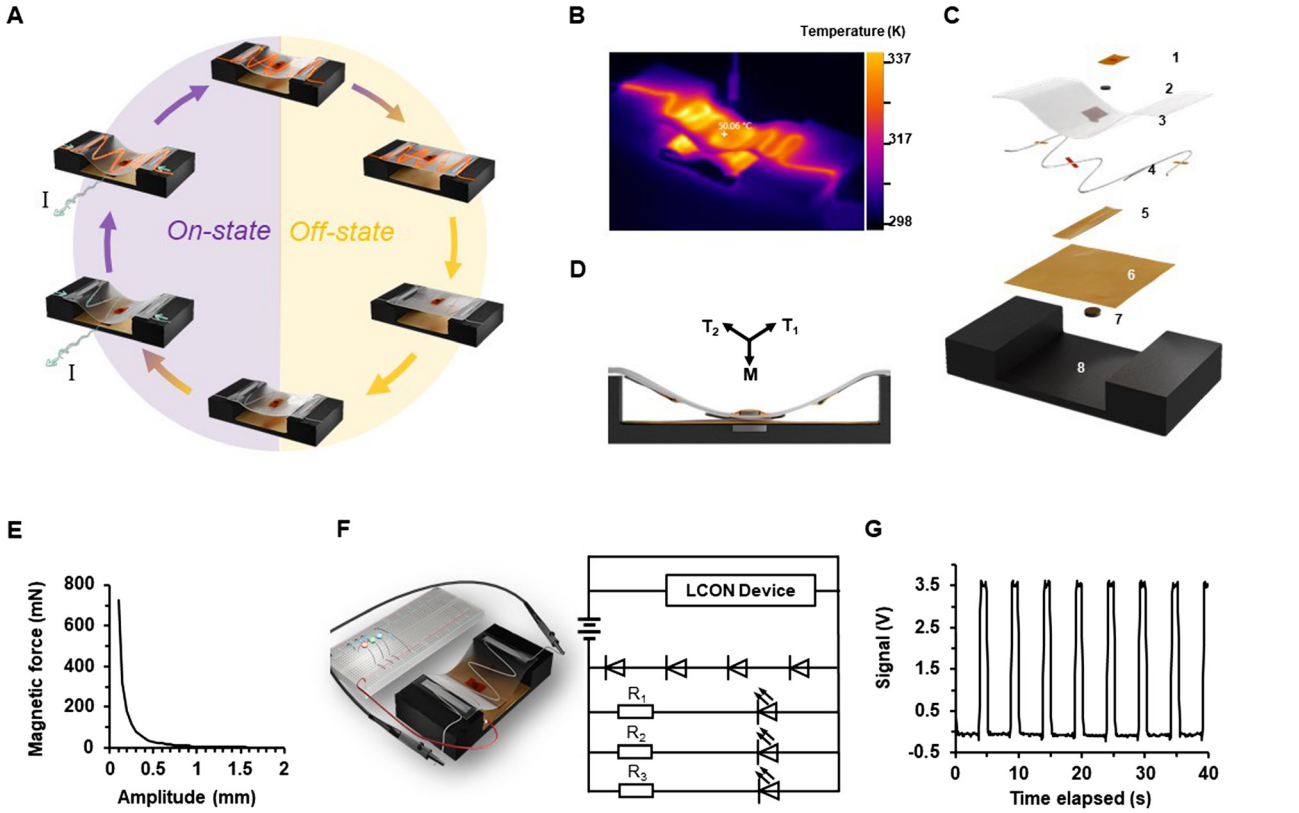

Fig. 1 Function and set-up of the LCON self-regulating oscillator. (A) 3-D Illustration of the feedback-loop cycle of the LCON self-regulating oscillator. (B) IR camera image of the LCON self-regulating oscillator in operation. (C) 3-D illustration of the dissection of the LCON self-regulating oscillator, displaying the (1) film magnet Kapton tape, (2) film magnet, (3) actuating film, (4) nichrome wiring and Kapton tape fasteners, (5) film copper tape, (6) platform copper tape, (7) platform magnet and (8) oscillator platform. (D) Schematic representation and 3-D illustration of the forces acting on the LCON self-regulating oscillator during the on-state. (E) Graphical representation of the magnetic attraction between mounted magnets within the LCON self-regulating oscillator. (F) Schematic representation and 3-D illustration of the simple hybrid circuit set-up for the LCON self-regulating oscillator. (G) Example of the signal generated by the operation of the LCON self-regulating oscillator within a circuit.

(FLCF) of the oscillator was shown to be tuneable between approximately 0.08 Hz and 0.87 Hz by adjusting its design or operation parameters. Yet, once a certain FLCF is set, it was observed to remain constant for all 50 tested configurations, translating to approximately 11 520 oscillations per sample over a total test time of 4 hours. An expected standard deviation of 3.22% was caused by random errors in the set-up or from the environment. This error was calculated by comparing the periods of all wavelengths over an oscillator operation time of 4 minutes for each configuration. The rare occurrence of major anomalies thus led to an inflation of the final error figure. Hence, despite the error value, periods of FLCF deviation of under 0.5% were also recorded. Moreover, upsetting the dynamic equilibrium of the system, such as through pushing the film down onto the oscillator platform to cause extended heating, only affects the FLCF temporarily. After the disturbance, the FLCF changes slightly each cycle until it reaches the initial value. Over the 6 months of testing, the only recorded errors originate from movement in the clamps on the oscillator platform after extended use. The consistency of the FLCF is regulated entirely by the stimuli-responsive actuation of the LCON film and acts as a testament to its self-regulating capacity.

Actuation principles and film characterization

The self-regulating properties of the LCON film originate from the changes in the molecular order of its constituent reactive mesogens. This is typical of a liquid crystal structure where, in the case of LCONs, it can be visualized as oligomerized reactive mesogens forming a ''crystal'' order within the ''liquid'' chain-extender matrix. (Fig. 2A) Each of our samples had different cross-linker and chain-extender contents to vary their mechanical properties. (Fig. 2B) Order within the LCONs is achieved by mechanical straining, aligning the reactive mesogens with the straining direction. In the case of our LCON films, all samples were strained to 200% in opposite directions along one axis to introduce planar molecular alignment along the straining director. (Fig. 2A) This stretched state is then arrested by photopolymerization to induce cross-linking between oligomers. As the synthesis of the LCON film is based on the Michael thiol-addition reaction, the absence of absorption peaks for thiol functional groups at wavenumbers 2600–2550 cm^{-1} in FTIR analysis verifies the cross-linker has been fully reacted within the polymerized structure.[33] (Fig. 2C) Reducing the order, or alignment, of the reactive mesogen through various stimuli leads to internal stresses and subsequent dimensional changes and within the LCON. As a result, the material experiences a

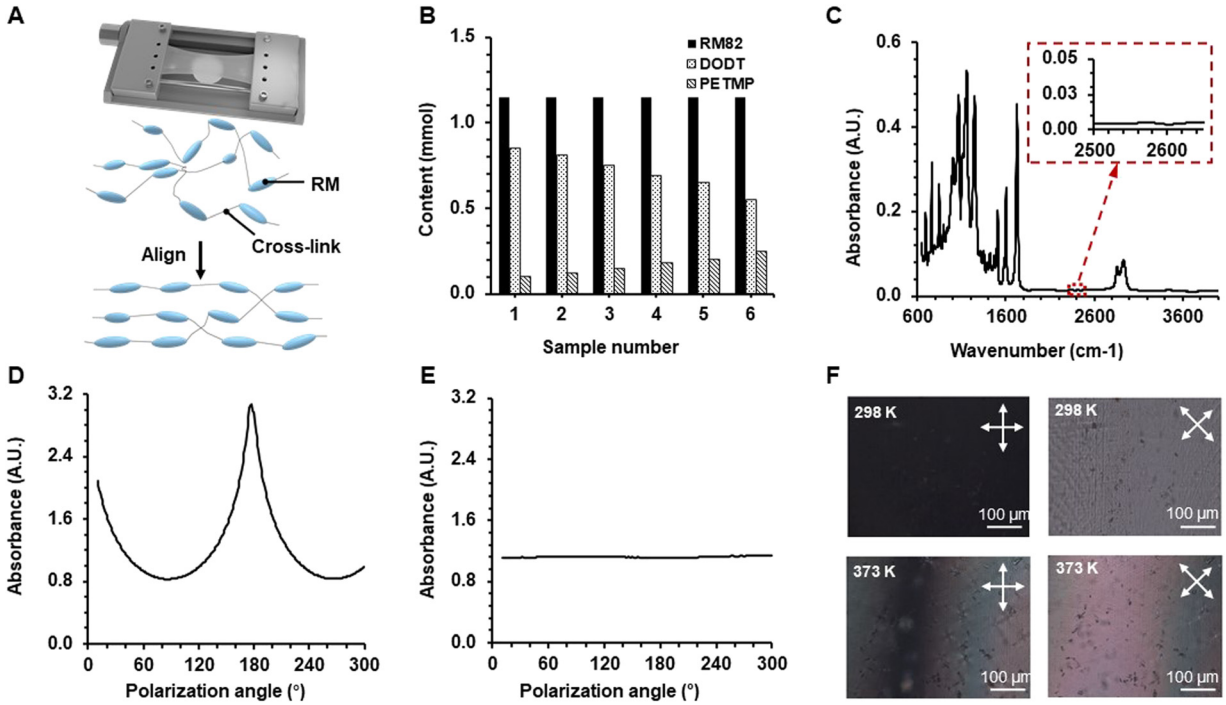

Fig. 2 Chemistry and actuation mechanisms of the LCON free-film samples. (A) 3-D visualization of the custom alignment device in operation and the schematic illustration of the liquid crystal structure within LCON samples and its aligned and non-aligned states. (B) Graphical representation of the chemical compositions of the LCON samples used to build the self-regulating oscillators. Analysis of a typical LCON free-film sample, in this case Sample 3: (C) FT-IR data and (D) graphical representation of the absorbance of dichroic-dye-doped LCON free-film at different polarization angles; temperatures were kept constant at approximately 298 K. (E) Graphical representation of the absorbance of dichroic-dye-doped LCON free-film at different polarization angles; temperatures were kept constant at 363 K. (F) Annotated POM images the LCON free-film samples at different crossed-polarizer angles and temperatures. The scale bars for each of the images represents 100 microns.

contraction in the director of the reactive mesogen alignment and expansion perpendicular to this director. This is the underlying principles for the stimuli-responsive actuation of LCONs. Moreover, the cross-linking within the liquid crystal structure of LCONs induces molecules to adopt the original ordered state when the actuation stimuli is removed, which enables this actuation to also be reversible.[34]

In the case of our oscillator, a thermal stimulus is applied to activate the actuation of the LCON film. The Joule effect from passing current through nichrome wire is utilized to achieve LCON actuation *via* an electrically-powered and electrically-controllable method. This allows the oscillator to be used as a component within a hybrid electrical circuit. The change in order caused by the applying Joule effect heating was quantified using crossed-polarizers optical microscopy (POM) and UV-vis spectrometer data. (Fig. 2D–F) These analyses recorded a change in order parameter, a quantification tool for liquid crystal order,[35] from 0.474 at 298 K to 0.027 at 363 K (Fig. S3, ESI†).

Critical actuation temperature

The temperature-dependent actuation of the LCON film implies that the on- and off-state switching of the oscillator is also temperature-dependent. Fundamentally, there will be an LCON film temperature at which the internal tension will be sufficient to overcome the switching threshold force. This critical actuation temperature was recorded for LCONs films with varying chemistry, namely with different degrees of cross-linking due to the varied ratios of di:tetra chain-extender. A greater ratio of tetra chain-extender leads to more cross-linking, while a greater ratio of di chain-extender results in less cross-linking. Dynamic mechanical thermal analysis (DMTA) of the LCON actuation forces with temperature showed that all films have a similar critical actuation temperature of approximately 339.2 K, despite having different degrees of cross-linking. Only 1.06% to 1.42% deviation of the critical actuation temperature of the films from the average was recorded. (Fig. 3A) This is hypothesized to be due to the oligomer chains within each LCON sample being the same length, as the thiol:acrylate ratio is constant for each sample. As a result, the responses of the LCON film to temperature would be expected to be similar, with similar internal stresses being produced due to the loss in order. In fact, the deviation in critical actuation temperatures may be due to possible measurement errors or random errors in the thiol:acrylate ratio during the synthesis process. Yet, the varying degree of crosslinking is observed to influence the overall rigidity of the film. DMTA data showed that LCON films with higher degrees of cross-linking have greater elastic moduli than LCON films with less cross-linking. (Fig. 3B) This increase in rigidity factor was confirmed through differential scanning calorimetry (DSC) analysis, where, despite similar thermal properties, the temperature transitions observed in less rigid LCON samples seemed gradually repressed for more rigid LCON samples. (Fig. 3C) We hypothesize

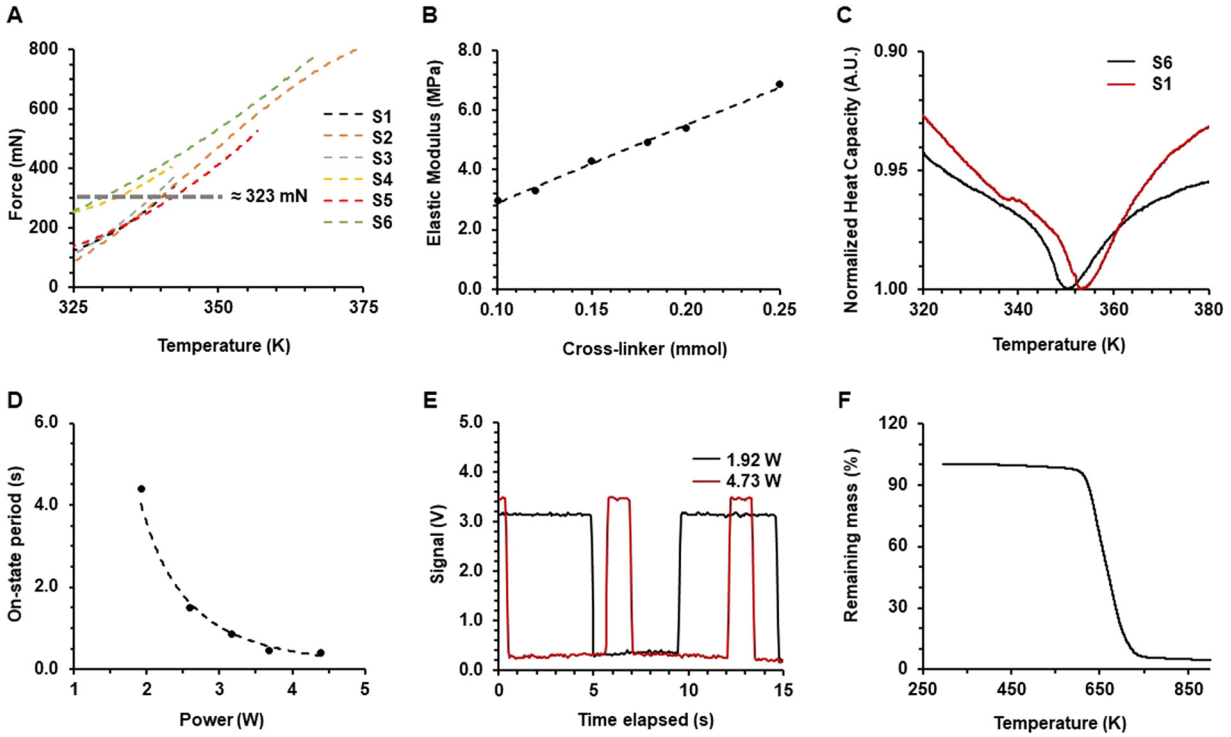

Fig. 3 Critical actuation behaviours based on chemistry and supplied power. (A) Graphical representation of actuation force with temperature for all LCON samples (S1–S6). (B) Graphical representation of the influence of cross-linker in an LCON sample on its elastic modulus. (C) Graphical representation of the focal temperature-based transition in the rigid sample 6 (S6) and compliant sample 1 (S1) LCON films. (D) Graphical representation of the influence of supplied power on the on-state period of the sample 3 LCON film oscillator. (E) Graphical comparison of the signals of the oscillator using the same sample 3 LCON film with 1.92 W and 4.73 W of powers. (F) Graphical representation of the thermal stability of a typical LCON sample through TGA.

that these transitions were suppressed due to the inability of reactive mesogens to move into their desired states.

Tuning the on-state

The presence of the critical actuation temperature indicates that tuning of the FLCF is possible by altering the rate at which the LCON film is heated. As our oscillator is a part of an electrical circuit, this can be easily achieved by varying the supplied power. Fundamentally, increasing the power supplied to the oscillator allows the LCON film to reach its critical actuation temperature quicker, exponentially decreasing the time the oscillator spends at its on-state and *vice versa*. (Fig. 3D) The hard phase difference between the off- and on-states of the oscillator allow, in this case, the on-state to be tuned individually to the off-state. (Fig. 3E and Fig. S2, ESI†) This demonstrates flexibility in the self-regulating properties of the LCN. Essentially, regardless of how high the heating rate of the LCON film is, the film temperature cannot exceed the critical actuation temperature. Moreover, thermal gravimetric analysis (TGA) has shown LCON stability at the critical actuation temperatures, meaning that a high heating rate would not damage the LCON film. (Fig. 3F) This provides evidence of oscillator durability and promises sustained self-regulation.

However, despite having the same effect on the on-state period of all the LCON samples, it is apparent that increasing the power supplied to the device has a greater impact on overall FLCF for higher rigidity films than for lower rigidity films. (Fig. 4A) As we established that power independently influences the on-state, it implies that the off-state has a more complex behaviour that also affects the on-state period itself.

Tuning the off-state

Fundamentally, the off-state period of the oscillator is dictated by the cooling rate, which ultimately leads to LCON film relaxation and reconnection to the oscillator platform to switch the system back to the on-state. Therefore, the off-state period can simply be varied by altering the cooling rate, for instance by changing the environmental temperature. On the other hand, the complex behaviour of the off-state is related to LCON film relaxation not experiencing the same sudden "snap-out" that it experienced during heating in the device on-state. Therefore, the off-state period is strongly related to the LCON film oscillation amplitude. (Fig. 4B) The greater the LCON film oscillation amplitude, the greater the time the film will spend cooling in the device off-state and *vice versa*. This directly affects the FLCF of the device. (Fig. 4C) Yet, the LCON film oscillation amplitude will also influence the post-critical actuation temperature at which the oscillator will switch back to its on-state. Depending on how low the post-critical actuation temperature of the LCON film is, the more heating it will require in the oscillator on-state until it will reach its critical actuation temperature again. As a result, the LCON film

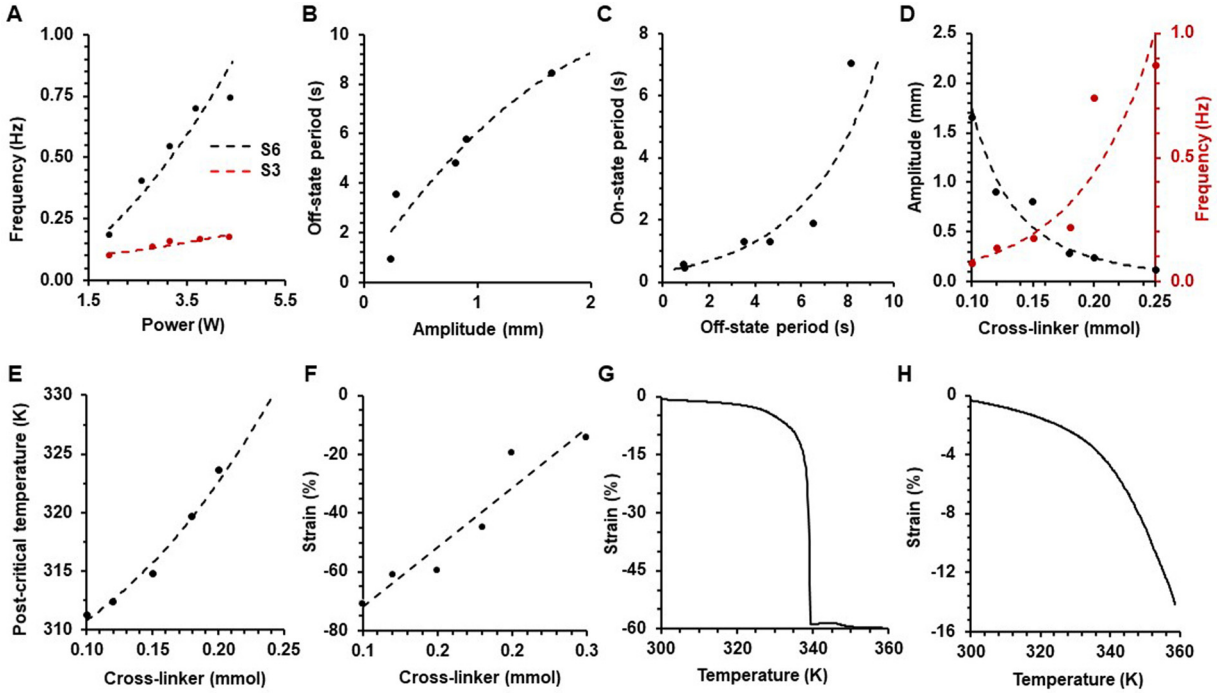

Fig. 4 Device FLCF behaviours based on power supplied, oscillation amplitude and LCON strain. (A) Graphical comparison of the influence of device power on the FLCF of LCON films of different rigidities (less rigid S3 and more rigid S6). (B) Graphical representation of the influence of film oscillation amplitude on oscillator off-state period. (C) Graphical representation of the influence of oscillator off-state period on oscillator on-state period. (D) Graphical comparison of the influence of LCON film cross-linker content on both film oscillation amplitude and FLCF of the oscillator. (E) Graphical representation of the influence of LCON film cross-linker content on the oscillator post-critical temperature. (F) Graphical representation of the influence of LCON film cross-linker content on the maximum actuation strain of the film. (G) Graphical representation of the actuation strain of the moderately-compliant sample 3 LCON film. (H) Graphical representation of the actuation strain of the rigid sample 6 LCON film.

oscillation amplitude not only affects the off-state but also affects the on-state. (Fig. 4C) Dissimilarities in the post-critical actuation temperature of the oscillator made with different LCON samples hence indicate that the oscillation amplitudes of the films differ based on LCON chemistry. (Fig. 4D and E) This would provide an explanation for the supplied power seemingly influencing the FLCF of oscillators with stiffer films more than that of oscillators with less stiff films.

Strain and post-critical actuation

Less rigid LCON films are observed to produce greater oscillation amplitudes in device operation. This is related to the greater strain less-rigid LCON films experience to achieve the same internal tension as stiffer LCON films, regardless of the critical actuation temperature for all films being similar. (Fig. 3A and 4F) We hypothesize that this is due to the different degrees of molecular mobility and the corresponding stress, or actuation force, that is generated within the LCON film with different degrees of cross-linking. Yet, as all the LCON films were operated on the same oscillator platform with the same threshold set by the magnetic force, all the films needed to achieve the same actuation force to switch the oscillator to its off-states. Yet, as different strains correspond to the same actuation force with different degrees of cross-linking within the LCON film, the dimensions to which the film "snaps out" to once it reaches the critical actuation temperature is different for each film. Image analysis was used during the operation of the oscillator to determine the different oscillation amplitudes for each LCON film sample. The LCON film oscillation amplitude film was varied between approximately 0.12 and 1.65 mm with changing LCON chemistry in our experiments (Fig. 4C).

Due to our oscillator design, the greater strain the LCON film will experience will translate into a greater oscillation amplitude. In principle, the oscillation amplitude of the LCON film can be varied by altering its chemistry. Moreover, clear jumps in strain values are observed for less rigid films as the film temperature approaches an activation threshold of approximately 340 K. (Fig. 4G) This sudden strain increase becomes increasingly masked for more rigid films, which explains the greater difference in FLCF between stiffer and less stiff LCON films. (Fig. 4H) It is hypothesized that this relates to greater cross-linking limiting molecular mobility and subsequently the maximum strain of the LCON.

Magnetic threshold

Beyond the material chemistry of the LCON film, the FLCF can also be altered by changing the pivotal critical actuation temperature. This can be achieved by simply altering the 323 mN default force of attraction between the mounted magnets in the current oscillator configuration. Increasing the magnetic force would increase the required LCON film internal tension and corresponding critical actuation temperature, and

vice versa. Essentially, the critical actuation temperature is determined by the pre-load applied on the LCON film, which can, very interestingly, be a force other than attraction between mounted magnets. For instance, this can be a load applied by a product in an automated quality control line, where the quality of the product is determined by its weight. Yet, further research is required to fully quantify the effect of this phenomena on FLCF to produce an accurate LCON-based weight sensor.

Conclusions

We have demonstrated the self-regulating properties of LCONs in an electrically-driven oscillator, where the LCON acts as a composite actuating sensor and a reconnectable circuit-breaker. The finely-tuneable self-regulation properties of the LCON films were exhibited by the readily adjustable FLCF and free-film oscillation amplitude of the device. Meanwhile, the engineered electrical conductivity of the LCON/nichrome composites allows for hybrid circuit designs and applications within the current electrical infrastructure of typical devices. Our LCON films combine the robotic functions of load-bearing, actuation, sensing and control into one material, potentially offering solutions for applications in need of complex self-regulation and inspiring innovation in device design. Thereby, our LCON oscillator could be applied in a variety of fields, ranging from automated control and medical applications to robotic systems, including haptics and self-cleaning surfaces. Therefore, our research delves into the material-to-device transition of LCONs by showcasing its unique applications based on its intrinsic properties. It is also important to note LCON films tested in our work were of the same dimensions; LCON samples of smaller dimensions were observed to achieve higher FLCFs, yet the full extent of this phenomenon must be quantified in further research towards miniaturizing the current system. We aspire to inspire further innovations for our materials in the soft robotics field, towards building miniaturized single-material electronic soft robots.

Experimental

Materials

RM82 (LC monomer, Daken Chemical), pentaerythritol tetrakis (3-mercaptopropionate) (tetra-thiol crosslinker, Bruno Bock Chemische Fabrik GmbH & co. KG), 2,2′-(ethylenedioxy) diethanethiol (di-thiol crosslinker, Sigma-Aldrich), dipropyl amine (Michael-addition catalyst, Sigma-Aldrich), and (Irgacure 651) 2,2-dimethoxy-1,2-diphenylethan-1-one (photocuring agent, Ciba Spezialtaetenchemiz AG) were all used as received to synthesize LOCN films. Dicholoromethane (solvent, Biosolve) was used as the solvent to facilitate the desired chemical reactions. Nichrome wire (heating element, Evek) was used to electrically-functionalize the LCON samples. 1-(4-((4-((4-Butylphenyl)diazenyl)phenyl) diazenyl) phenyl)pyrrolidine, commercially known as G-205 (Dichroic dye, Hayashibara Biochemical Laboratories Inc.), was used in the procedure to measure order parameter of LCON films.

Synthesis of polydomain LCONs

RM82 (755.28 mg, 1.15 mmol), pentaerythritol tetrakis(3-mercaptopropionate) (73.30 mg, 0.15 mmol), 2,2′-(ethylenedioxy)diethanethiol (136.73 mg, 0.75 mmol) and photoinitiator (1 wt%) were first dissolved in DCM (5.00 mL), forming the monomer and crosslinker solution. The diothiol:tetrathiol ratio in this monomer and crosslinker solution was varied between samples to test the influence of material chemistry on the final device. This solution is then poured into a Teflon mould (Fig. S4, ESI†). 7.44 mg dipropyl amine was dissolved into 1.00 mL DCM solution, forming the catalysis solution. These solutions were then also added to the custom-made Teflon mould and the mixtures were then shaken to promote dispersion. Polydomain LCONs were obtained by drying the solution at room temperature overnight.

Fabrication of LCON actuators

Monodomain LCONs with homogeneous planar orientation were produced by stretching polydomain LCONs at the strain of 200% on a custom stretching device. The stretched material was then exposed to UV irradiation (100 mW cm^{-2}) for 10 minutes to trigger the photo-initiator and cross-polymerize the material, arresting the molecular alignment within the film. The film was flipped halfway through the polymerization to ensure the material was uniformly photopolymerized. The planar molecular orientation within the LCON enables contraction along its director upon actuation.

Characterization of LCONs

Dynamic scanning calorimetry (DSC, TA instruments Q2000) was performed at a scanning rate of 10 °C min^{-1} between −50 °C and 120 °C. Tensile strain–stress test was performed through dynamic mechanical thermal analysis (DMTA, TA instruments Q800) apparatus at room temperature. This apparatus was also used to measure actuation stress and strain separately between 20 °C and 80 °C. Actuation force was further quantified using a custom-build device (Fig. S5, ESI†). The thermal stability of monodomain LCNs was measured through Thermogravimetric analysis (TGA, TA instruments Q500) under air atmosphere and repeated in nitrogen atmosphere. Ultraviolet-visible (UV-vis spectroscopy, PerkinElmer UV/vis/NIR Lambda 750) spectroscopy (performed on a G205-integrated LCON film) and crossed-polarizer optical microscopy (POM, Leica DM6000M) data is recorded to calculate molecular alignment in LCONs. Fourier-transform Infra-red spectroscopy (FTIR spectroscopy, Varian 670-IR FTIR spectrometer) was performed to verify the chemical composition of the final LCON films.

Device set-up

Polylactic acid was used to 3-D print (Filament extrusion 3-D printer, Ultimaker S5) the device platforms and conductivity was induced by applying copper tape. Magnets (NdFeB, Supermagnete) were placed in the device platform and adhered onto the LCON film to ensure electrical contact. An LCON film with dimensions of 25 mm × 10 mm × 0.3 mm was cut for the

typical device. Copper tape was also placed on the contacting surface of the LCON film to reduce contact resistance. Nichrome wire with a diameter of 0.05 mm (80% Ni/20% Cr, Evek) was fastened to the contacting surface of the LCON with Kapton tape. The nichrome tape was bent into a waveform-like pattern to increase covered film surface and allow for free-movement during LCON actuation. Constant force was applied on the edges of LCON film using clamps. The device was integrated into a test circuit consisting of a power supply (Tenma 72-2720), 4 Diodes (Onsemi MUR120RLG), 3 Light-Emitting-Diodes (eBoot LN0628) and 3 100 Ohm resistors with 5% tolerance (VITROHM PO595-05T100R).

Characterization of feedback loop and self-regulation

As the device is electrically-powered, the voltage profile within the device was measured over time using an oscilloscope (RTB2004, Rohde & Schwarz) to accurately determine the device operation frequency. The amplitude of free-film oscillation was determined by computer analysis of video footage of the device in operation (MATLAB). 8 V of potential difference was initially applied across the circuit, but this voltage was varied during experimentation to gauge the effect of power on device properties.

Author contributions

D. L. conceived the research and supervised the project. M. O. A. conducted experiments, analysed the data, and drafted the manuscript. J. P. performed the image analysis from experiments. P. L. aided M. O. A. in the use of a custom set-up to measure actuation force of LCON films in operation. M. O. A., P. L. and D. L. contributed to the writing of manuscript.

Conflicts of interest

There are no conflicts to declare.

Acknowledgements

We thank the Netherlands Organization for Scientific Research (NWO OCENW.KLEIN. 10854, START-UP 8872), NWO Sectorplan and the European Union's Horizon 2020 Research and Innovation Programme under the Marie Sklodowska-Curie Grant Agreement No. 956150 (STORM-BOTS) for financial support. We thank Deniz Astam for her help in applying Visual Basic code for our data analysis. We also wish to thank Dr Thierry K. Slot for his help in planning circuit configurations for our LCON self-regulating oscillation device. We finally thank Dr John S. Biggins for his motto of "make the material the machine", as it inspired our narrative for our research.

Notes and references

1 L. Kromann, N. Malchow-Møller, J. R. Skaksen and A. Sørensen, Automation and productivity—a cross-country, cross-industry comparison, *Ind. Corp. Chang.*, 2020, **29**, 265–287.
2 R. Aron, S. Dutta, R. Janakiraman and P. A. Pathak, The impact of automation of systems on medical errors: Evidence from field research Information Systems Research, *Inf. Syst. Res.*, 2011, **22**, 429–446.
3 M. M. Moya and H. Seraji, Robot control systems: A survey, *Robotics*, 1987, **3**, 329–351.
4 S. Khan and W. Jehangir, Evolution of Artificial Hearts: An Overview and History, *Cardiol. Res.*, 2014, **5**, 121.
5 N. M. Amosov, V. A. Lishchuk and B. L. Palets, Self-regulation of the heart, *Math. Biosci.*, 1969, **5**, 205–226.
6 D. E. Jaroszewski, E. M. Anderson, C. N. Pierce and F. A. Arabia, The SynCardia freedom driver: A portable driver for discharge home with the total artificial heart, *J. Heart and Lung Transplant*, 2011, **30**, 844–845.
7 J. Y. Kresh and J. A. Armour, The heart as a self-regulating system: integration of homeodynamic mechanisms, *Technol. Health Care*, 1997, **5**, 159–169.
8 A. O. Gorbach and R. v Bubnov, Study of the digital model of self-regulation system of the heart, *EPMA J.*, 2014, **5**, A89.
9 D. Horvath, N. Byram, J. H. Karimov, B. Kuban, G. Sunagawa, L. A. R. Golding, N. Moazami and K. Fukamachi, Mechanism of Self-Regulation and In Vivo Performance of the Cleveland Clinic Continuous-Flow Total Artificial Heart, *Artif. Organs*, 2017, **41**, 411–417.
10 Y. Zhan, G. Zhou, B. A. G. Lamers, F. L. L. Visschers, M. M. R. M. Hendrix, D. J. Broer and D. Liu, Artificial Organic Skin Wets Its Surface by Field-Induced Liquid Secretion, *Matter*, 2020, **3**, 782–793.
11 X. Yang, H. Li, X. Zhao, W. Liao, C. X. Zhang and Z. Yang, A novel, label-free liquid crystal biosensor for Parkinson's disease related alpha-synuclein, *Chem. Commun.*, 2020, **56**, 5441–5444.
12 L. Ceamanos, Z. Kahveci, M. Lopez-Valdeolivas, D. Liu, D. J. Broer and C. Sanchez-Somolinos, Four-dimensional printed liquid crystalline elastomer actuators with fast photoinduced mechanical response toward light-driven robotic functions, *ACS Appl. Mater. Interfaces*, 2020, **12**, 44195–44204.
13 O. M. Wani, H. Zeng and A. Priimagi, A light-driven artificial flytrap, *Nat. Commun.*, 2017, **8**, 15546.
14 K. Fukuhara, S. Nagano, M. Hara and T. Seki, Free-surface molecular command systems for photoalignment of liquid crystalline materials, *Nat. Commun.*, 2014, **5**, 1–8.
15 M. Yang, Y. Xu, X. Zhang, H. K. Bisoyi, P. Xue, Y. Yang, X. Yang, C. Valenzuela, Y. Chen, L. Wang, W. Feng, Q. Li, M. Yang, X. Zhang, P. Xue, Y. Yang, X. Yang, C. Valenzuela, Y. Chen, L. Wang, W. Feng, Y. Xu, Q. Li and H. K. Bisoyi, Bioinspired Phototropic MXene-Reinforced Soft Tubular Actuators for Omnidirectional Light-Tracking and Adaptive Photovoltaics, *Adv. Funct. Mater.*, 2022, **32**, 2201884.
16 D. J. Broer, J. Lub and G. N. Mol, *Nature*, 1995, **378**, 467–469.
17 D. Cuypers, H. de Smet and A. van Calster, VAN LCOS Microdisplays: A Decade of Technological Evolution, *J. Disp. Technol.*, 2011, **7**, 127–134.

18 M. O. Astam, Y. Zhan, T. K. Slot and D. Liu, Active Surfaces Formed in Liquid Crystal Polymer Networks, *ACS Appl. Mater. Interfaces*, 2021, **14**(20), 22697–22705, DOI: **10.1021/acsami.1c21024**.

19 N. Zettsu, T. Ogasawara, N. Mizoshita, S. Nagano and T. Seki, Photo-Triggered Surface Relief Grating Formation in Supramolecular Liquid Crystalline Polymer Systems with Detachable Azobenzene Unit, *Adv. Mater.*, 2008, **20**, 516–521.

20 J. Ma, Y. Yang, C. Valenzuela, X. Zhang, L. Wang and W. Feng, Mechanochromic, Shape-Programmable and Self-Healable Cholesteric Liquid Crystal Elastomers Enabled by Dynamic Covalent Boronic Ester Bonds, *Angew. Chem., Int. Ed.*, 2022, **61**, e202116219.

21 L. T. de Haan, V. Gimenez-Pinto, A. Konya, T.-S. Nguyen, J. M. N. Verjans, C. Sánchez-Somolinos, J. V. Selinger, R. L. B. Selinger, D. J. Broer, A. P. H. J. Schenning, L. T. de Haan, J. M. N. Verjans, D. J. Broer, A. P. H. J. Schenning, V. Gimenez-Pinto, A. Konya, T. S. Nguyen, J. V. Selinger, R. L. B. Selinger and C. Sánchez-Somolinos, Accordion-like Actuators of Multiple 3D Patterned Liquid Crystal Polymer Films, *Adv. Funct. Mater.*, 2014, **24**, 1251–1258.

22 A. Konya, V. Gimenez-Pinto and R. L. B. Selinger, Modeling Defects, Shape Evolution, and Programmed Auto-Origami in Liquid Crystal Elastomers, *Front*, *Mater. Sci.*, 2016, **3**, 24.

23 A. Lancelot, T. Sierra and J. L. Serrano, Nanostructured liquid-crystalline particles for drug delivery, *Expert Opin. Drug Delivery*, 2014, **11**, 547–564.

24 M. B. Ros, J. L. Serrano, M. R. de La Fuente and C. L. Folcia, Banana-shaped liquid crystals: a new field to explore, *J. Mater. Chem.*, 2005, **15**, 5093–5098.

25 J. Wang, S. Huang, Y. Zhang, J. Liu, M. Yu and H. Yu, Hydrogen Bond Enhances Photomechanical Swing of Liquid-Crystalline Polymer Bilayer Films, *ACS Appl. Mater. Interfaces*, 2021, **13**, 6585–6596.

26 C. Shen, R. Lan, R. Huang, Z. Zhang, J. Bao, L. Zhang and H. Yang, Photochemically and photothermally controllable liquid crystalline network and soft walkers, *ACS Appl. Mater. Interfaces*, 2021, **13**, 3221–3227.

27 S. Ma, X. Li, S. Huang, J. Hu and H. Yu, A Light-Activated Polymer Composite Enables On-Demand Photocontrolled Motion: Transportation at the Liquid/Air Interface, *Angew. Chem.*, 2019, **131**, 2681–2685.

28 W. Liao and Z. Yang, The Integration of Sensing and Actuating based on a Simple Design Fiber Actuator towards Intelligent Soft Robots, *Adv. Mater. Technol.*, 2022, **7**, 2101260.

29 J. Hu, W. Wang and H. Yu, Endowing Soft Photo-Actuators with Intelligence, *Adv. Intell. Syst.*, 2019, **1**, 1970081.

30 J. Wang, B. Yang, M. Yu and H. Yu, Light-Powered Self-Sustained Oscillators of Graphene Oxide/Liquid Crystalline Network Composites Showing Amplitude and Frequency Superposition, *ACS Appl. Mater. Interfaces*, 2022, **14**, 15632–15640.

31 J. Wang, T. Song, Y. Zhang, J. Liu, M. Yu and H. Yu, Light-driven autonomous self-oscillation of a liquid-crystalline polymer bimorph actuator, *J. Mater. Chem. C*, 2021, **9**, 12573–12580.

32 G. N. Mol, K. D. Harris, C. W. M. Bastiaansen and D. J. Broer, Thermo-Mechanical Responses of Liquid-Crystal Networks with a Splayed Molecular Organization, *Adv. Funct. Mater.*, 2005, **15**, 1155–1159.

33 M. O. Saed, A. H. Torbati, D. P. Nair and C. M. Yakacki, Synthesis of Programmable Main-chain Liquid-crystalline Elastomers Using a Two-stage Thiol-acrylate Reaction, *J. Vis. Exp.*, 2016, 53546.

34 D. J. Broer and G. N. Mol, Anisotropic thermal expansion of densely cross-linked oriented polymer networks, *Polym. Eng. Sci.*, 1991, **31**, 625–631.

35 R. G. Horn, Refractive indices and order parameters of two liquid crystals, *J. Phys. France*, 1978, **39**, 105–109.

